Optical magnetometer array for fetal magnetocardiography

Robert Wyllie,[1] Matthew Kauer,[1] Ronald T. Wakai,[2] and Thad G. Walker[1,*]

[1]*Department of Physics, University of Wisconsin–Madison, 1150 University Avenue, Madison, Wisconsin 53706, USA*

[2]*Department of Medical Physics, University of Wisconsin–Madison, 1111 Highland Avenue, Madison, Wisconsin 53705, USA*

**Corresponding author: tgwalker@wisc.edu*

Received February 22, 2012; revised March 27, 2012; accepted March 28, 2012;
posted March 30, 2012 (Doc. ID 163553); published June 6, 2012

We describe an array of spin-exchange-relaxation-free optical magnetometers designed for detection of fetal magnetocardiography (fMCG). The individual magnetometers are configured with a small volume with intense optical pumping, surrounded by a large pump-free region. Spin-polarized atoms that diffuse out of the optical pumping region precess in the ambient magnetic field and are detected by a probe laser. Four such magnetometers, at the corners of a 7 cm square, are configured for gradiometry by feeding back the output of one magnetometer to a field coil to null uniform magnetic field noise at frequencies up to 200 Hz. We present the first measurements of fMCG signals using an atomic magnetometer.

OCIS codes: 170.4580, 280.1415.

Spin-exchange-relaxation-free (SERF) magnetometers [1,2] have comparable or better sensitivities as compared to superconducting (SQUID) magnetometers, without the cryogenics. These magnetometers have been configured as short baseline (~1 cm) gradiometers and used for detection of adult magnetoencephalography [3,4]. A sub-cubic-centimeter SERF magnetometer was recently used for adult magnetocardiography (MCG) and magnetorelaxometry [5]. We demonstrated a high-sensitivity SERF magnetometer array for adult MCG [6]. In this paper we report the first detection of fetal MCG (fMCG) using atomic magnetometers.

Biomagnetic applications require cancellation techniques, such as gradiometry, to reduce environmental interference, even in magnetically shielded rooms. A 25-detector array of M_x atomic magnetometers was recently used [7] to acquire adult MCG in a minimally shielded environment with ~100 $\mathrm{fT}/\sqrt{\mathrm{Hz}}$ sensitivity, an order of magnitude above the ~10 $\mathrm{fT}/\sqrt{\mathrm{Hz}}$ limit desired to detect 10× smaller fMCG signals. For fMCG, the fetal heart is typically located about 5–10 cm below the mother's skin, which should be equal to the gradiometer baseline for maximum signal-to-noise ratio gradiometry [8]. For such large detector separations, high-quality SERF gradiometry with a single laser beam is challenging due to inevitable gradients in pumping rates and AC Stark shifts that cause the frequency dependence of the response to vary across the probe laser volume, giving imperfect cancellation of uniform magnetic fields at all frequencies. A promising attack on this problem is to use active feedback from one or more channels to null the magnetic noise in a manner similar to [7].

In this Letter, we demonstrate a four-channel SERF magnetometer array with 7 cm channel spacing. The individual channels are operated in a diffusive SERF regime, where the atomic precession is detected outside the spatially localized optical pumping regions. Using this scheme, we demonstrate real-time detection of fMCG, a promising new method for diagnosing serious heart rhythm abnormalities in the fetus [9]. Signal processing from the four channels allows us to isolate the fMCG signal from the maternal MCG interference and to compare the waveform characteristics with those recorded on a commercial SQUID system. Finally, in order to combat spatially uniform magnetic interference, we operate the array configured as a set of gradiometers using active cancellation of the magnetic field detected by one of the channels and demonstrate 40 dB interference rejection.

The basic configuration of our SERF array is detailed in [6] and depicted in Fig. 1. Four magnetometers are located at the corners of a square, separated by 7 cm. In each channel, a 4 mW circularly polarized 795 nm pump laser beam with a waist of 0.05 cm optically pumps the atoms in the $\hat{z}$ direction at the center of a 1 cm square glass cell. Faraday rotation of a ~780 nm probe laser with a 0.3 cm waist detects the spin polarization P_x along the $\hat{x}$ direction that is produced by magnetic fields along the $\hat{y}$ direction (perpendicular to the plane of the array). When run as a hardware gradiometer, the signal P_{1x} from channel 1 of the array is amplified by a gain stage and fed back to a current source driving a single rectangular magnetic field coil in order to keep $P_{1x} = 0$. The four channels are symmetrically located in the plane of the feedback field coil so that uniform magnetic fields are cancelled at each

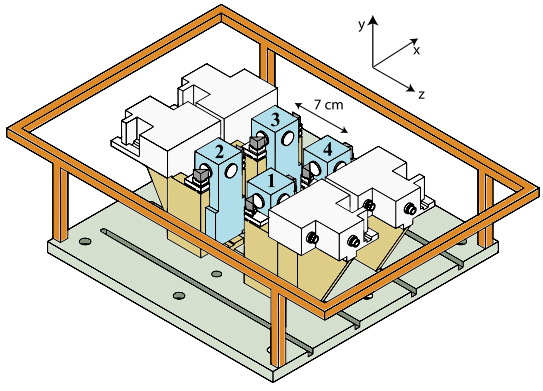

Fig. 1. (Color online) Biomagnetometer array. Four magnetometers are symmetrically located in the plane of a field coil. The output P_{1x} of one magnetometer is fed back to actively null B_{1y}. Each channel consists of a heated glass cell (numbered) and a fiber-coupled laser/detection module.

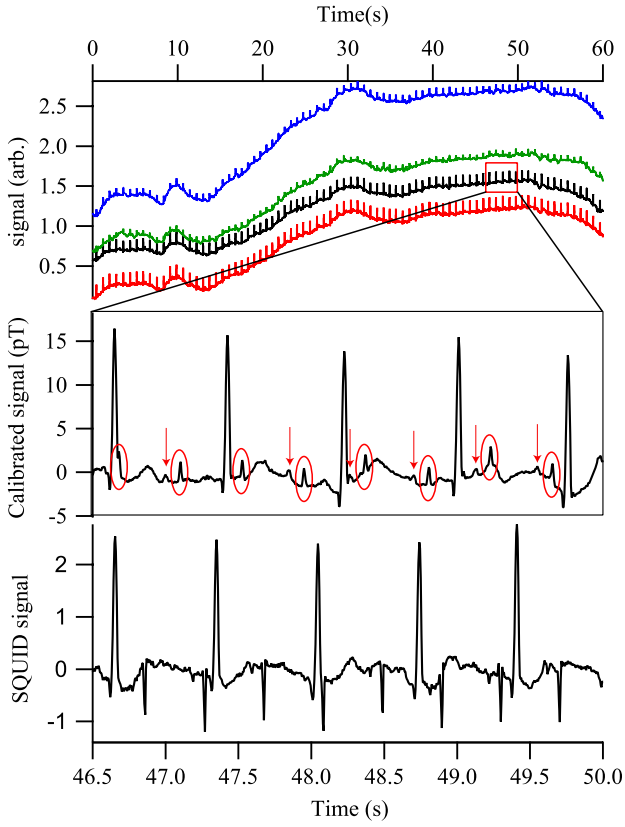

Fig. 2. (Color online) (Top) Real-time MCG from a 31 week fetus, showing all magnetometer channels. (Middle) Portion of channel 2, with an 80 Hz low-pass filter and a 60 Hz comb filter applied. The fetal QRS complexes are circled; arrows identify the fetal *P*-wave components. (Bottom) SQUID gradiometer signal with the same filters applied. The gradiometry suppresses the maternal MCG as compared to the fMCG.

channel. The signals in channels 2–4 are therefore gradiometric with respect to channel 1.

Since the probe laser is much larger than the pump laser and because the sensitivity is suppressed where the pump intensity is high, it primarily detects atoms that diffuse out of the pump beam region. The cells contain 50 torr of N_2 gas for excited-state quenching [10] and roughly 20 torr of He. The diffusion coefficient is estimated to be $D = 2.9$ cm/s. At 150 °C, we estimate that the effective spin-relaxation rate of the atoms is about $\Gamma' = 6.5$/s, including nuclear spin slowing-down effects [11]. Since the diffusion length $\Lambda = 2\pi\sqrt{D/\Gamma'} = 4.2$ cm is greater than the cell size, wall relaxation dominates spin relaxation in these cells. The large probe beam and localized pump means we are primarily detecting atoms in regions with reduced AC Stark shifts and pump-induced relaxation. Despite the relatively high wall relaxation rates in these cells (~85/s), our 5–10 fT/$\sqrt{\text{Hz}}$ ($f > 20$ Hz) single channel sensitivity is somewhat above the noise level of our shielded room.

We have used the SERF magnetometer array open loop to detect fMCG signals in real time. The array is placed with the $y = 0$ plane just above the abdominal skin and relatively centered over the fetus's position, with two of the channels closer to the mother's heart, and the other two further away. Figure 2 shows the raw

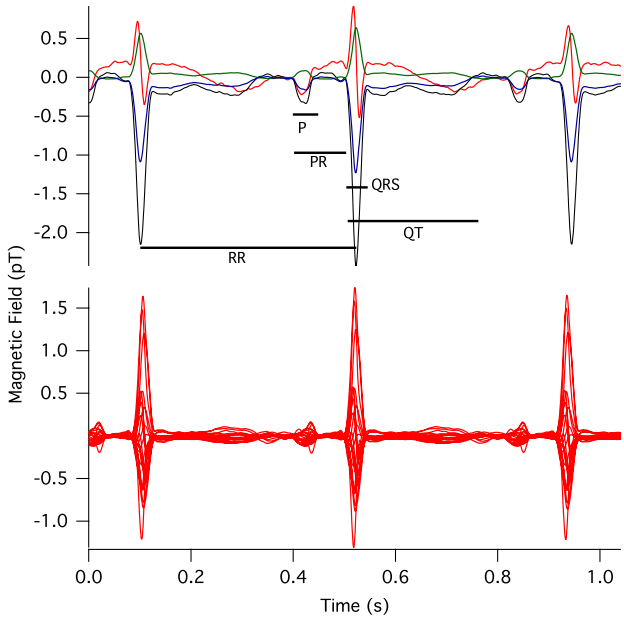

Fig. 3. (Color online) Comparison of the (top) prototype optical magnetometer and (bottom) commercial SQUID signals, with timings between features corresponding to Table 1.

signals observed from a fetus at 31 weeks gestation; the only filtering is a 80 Hz low-pass filter and a 60 Hz comb filter. The fetal QRS peaks are readily seen (circled in the blown-up portion of the signal) with sufficient signal-to-noise ratio to allow for the positioning of the detector to be adjusted to maximize the fetal signal in real time. Note that the *p*-wave components, denoted by arrows, are also readily observed. These are of particular importance for diagnosis of arrhythmias. [12]

The sensitivity of the raw fMCG tracings was similar for the SERF magnetometer and a seven-channel vector SQUID magnetometer (Tristan Vector Magnetometer, Tristan, Inc., San Diego) with 21 SQUID detectors. The SQUID time series was acquired about 10 min after the SERF time series. A spatial filter [13] was applied to isolate the fetal signal from the maternal interference, and averaged waveforms were computed using autocorrelation to time-align the fetal QRS complexes. Figure 3 shows the averaged fMCG waveforms obtained using the two magnetometers, and Table 1 shows a comparison of waveform interval measurements. The intervals measured with the SERF and SQUID systems show excellent agreement.

In a hospital setting, large interfering background fields are often incompletely suppressed by the shielded room. In our case, a nearby ventilation fan (turned off in Fig. 2) is the largest interfering field. By running the array with feedback from one of the channels, we observe real-time fMCG even in the presence of such interference. Figure 4 shows the array run with feedback from channel

Table 1. Intervals between Various Components of the fMCG Waveforms in Milliseconds

Method	RR	PR	P	QRS	QT	QTc
SERF	425	95	42	47	264	405
SQUID	415	90	41	48	241	375

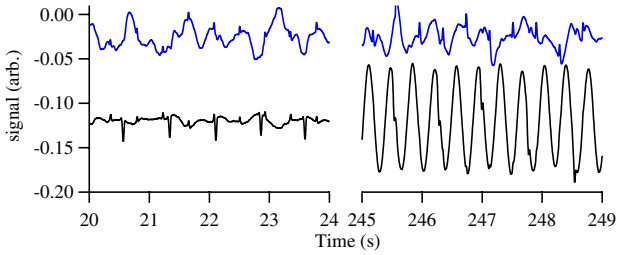

Fig. 4. (Color online) Two feedback scenarios. The lower trace is the current supplied to the large field coil to hold the signal constant at channel 4. The upper trace shows the field at another channel. (left) Data with a nearby ventilation fan off; the maternal signal is nearly the same size at the two channels, so it is largely absent from the upper channel. (right) With the fan on, the fMCG is still visible in the upper channel thanks to the feedback compensation.

4. The field from the fan dominates even the maternal MCG field in channel 4. Nevertheless, the feedback effectively cancels the interference in the other channels, and the fMCG signals are easily discerned. The interference is suppressed in the other channels by 40 dB. The gradiometric white noise is only slightly reduced from the single-channel white noise as the white noise in the individual channels is uncorrelated.

Although we have not yet done so, it would be advantageous to run the other channels of the array with self-feedback in order to linearize the phase and amplitude response. In this way, it should be possible to significantly improve the quality of the gradiometry.

Finally, we qualitatively discuss the diffusive SERF to illustrate its features. At high alkali densities, SERF magnetometers are optically thick, producing substantial pumping rate and AC Stark gradients inside the cell. Detecting atoms that have diffused out of a small pumping region allows reduced sensitivity to these effects. Other potential advantages of this configuration include reduced optics size, ease of pumping several cells with the same beam, and less stringent demands on pump laser stability. Many of these features are shared with atomic-beam Faraday–Ramsey magnetometry [14].

In conclusion, we have demonstrated that SERF magnetometers can be used for real-time fMCG detection and in an array can be used for spatial filtering of the maternal MCG signal for clinically interesting applications. We expect that these results can be substantially improved upon by adding feedback to all channels, by increasing the channel count (either by using more magnetometers or by introducing detection of multiple field components in each magnetometer via a parametric modulation scheme [15]), and by using vapor cells with better properties than those used here. From our perspective, the pieces are in place to make high-quality gradiometric SERF arrays with excellent sensitivity at a cost per channel significantly lower than SQUIDs.

This work was supported by the National Institutes of Health Eunice Kennedy Shriver National Institute of Child Health & Human Development, R01HD057965. The authors are solely responsible for the content. We appreciate help from Suhong Yu and Greg Smetana.

References

1. I. K. Kominis, T. W. Kornack, J. C. Allred, and M. V. Romalis, Nature **422**, 596 (2003).
2. W. Happer and A. C. Tam, Phys. Rev. A **16**, 1877 (1977).
3. H. Xia, A. B. A. Baranga, D. Hoffman, and M. V. Romalis, Appl. Phys. Lett. **89**, 211104 (2006).
4. C. N. Johnson, P. Schwindt, and M. Weisend, Appl. Phys. Lett. **97**, 243703 (2010).
5. S. Knappe, T. H. Sander, O. Kosch, F. Wiekhorst, J. Kitching, and L. Trahms, Appl. Phys. Lett. **97**, 133703 (2010).
6. R. Wyllie, M. Kauer, G. S. Smetana, R. T. Wakai, and T. G. Walker, Phys. Med. Biol. **57**, 2619 (2012).
7. G. Bison, N. Castagna, A. Hofer, P. Knowles, J. L. Schenker, M. Kasprzak, H. Saudan, and A. Weis, Appl. Phys. Lett. **95**, 173701 (2009).
8. V. Pizzella, S. D. Penna, C. D. Gratta, and G. L. Romani, Supercond. Sci. Technol. **14**, R79 (2001).
9. L. K. Hornberger and K. Collins, J. Am. Coll. Cardiol. **51**, 85 (2008).
10. B. Lancor and T. G. Walker, Phys. Rev. A **82**, 043417 (2010).
11. T. Walker and W. Happer, Rev. Mod. Phys. **69**, 629 (1997).
12. P. Kligfield, L. S. Gettes, J. J. Bailey, R. Childers, B. J. Deal, E. W. Hancock, G. van Herpen, J. A. Kors, P. Macfarlane, D. M. Mirvis, O. Pahlm, P. Rautaharju, and G. S. Wagner, Circulation **115**, 1306 (2007).
13. M. Chen, R. Wakai, B. VanVeen, and J. Perinat, J. Perinat. Med. **29**, 486 (2001).
14. D. Budker, W. Gawlik, D. F. Kimball, S. M. Rochester, V. V. Yashchuk, and A. Weis, Rev. Mod. Phys. **74**, 1153 (2002).
15. Z. Li, R. T. Wakai, and T. Walker, Appl. Phys. Lett. **89**, 134105 (2006).